Mem. S.A.It. Vol. 92, 71

Memorie della

Observation and Characterization of the Solar Turbulent Convection

G. Viavattene[1,2]

[1] Università degli Studi di Roma "Tor Vergata", Via della Ricerca Scientifica, 1, 00133 Rome, Italy
[2] Currently at: INAF - Osservatorio Astronomico di Roma, Via Frascati, 33, I-00078 Monte Porzio Catone, Italy, e-mail: giorgio.viavattene@inaf.it

Abstract. The turbulent solar magneto-convection is one of the most intriguing phenomena observed on our star and it presents several aspects that are not yet completely understood. In this work, the physical properties of the solar turbulent magneto-convection are studied using two complementary approaches: the analysis of a spectropolarimetric dataset and the design, development and realization of instrumentation for Solar Physics applications. Concerning the data analysis, I present a comparison of results from the application of different techniques to estimate the properties of the solar plasma and from the verification of the Gallavotti-Cohen Fluctuation Relation. For the instrumental development, three different activities are described, all aiming to improve the current tools to study the solar magneto-convection.

Key words. Solar Physics – Solar Turbulent Convection – Center-of-Gravity Method – Inversion Techniques – Gallavotti-Cohen Fluctuation Relation – Solar Spectropolarimetry – Fabry-Perot Interferometers – Optical Design – Magneto-Optical Filters – Solar Telescopes

1. Introduction: the Solar Convection

Convection due to vertical temperature gradient inside a gravitational field is one of the most frequent type of fluid motion in astrophysical environments and yet one of the most complex and poorly known because of its non-linear and non-local behaviour (Nordlund et al., 2009; Stein, 2012). In the Sun, the convection produces a large variety of phenomena that are observed in the solar atmosphere and it is of fundamental importance for the internal structure and appearance of the Sun. The simple Rayleigh-Beńard convection theory (Getling, 2001; Ching, 2014), used to describe the convective processes, is not sufficient to describe the high dynamics of the solar convection because this is a very peculiar case of convection for several reasons: 1) the downflow plasma of the solar convection is turbulent due to the high density stratification in the upper convection layer, which generates unstable and evolving convective cells; 2) the magnetic fields generated by the dynamo process permeate the whole solar surface, producing a perturbation of the Rayleigh-Beńard convection pattern; 3) the solar surface is a complex interface layer where there is a strong transition of the energy transport mode, from the convection of the lower layers to

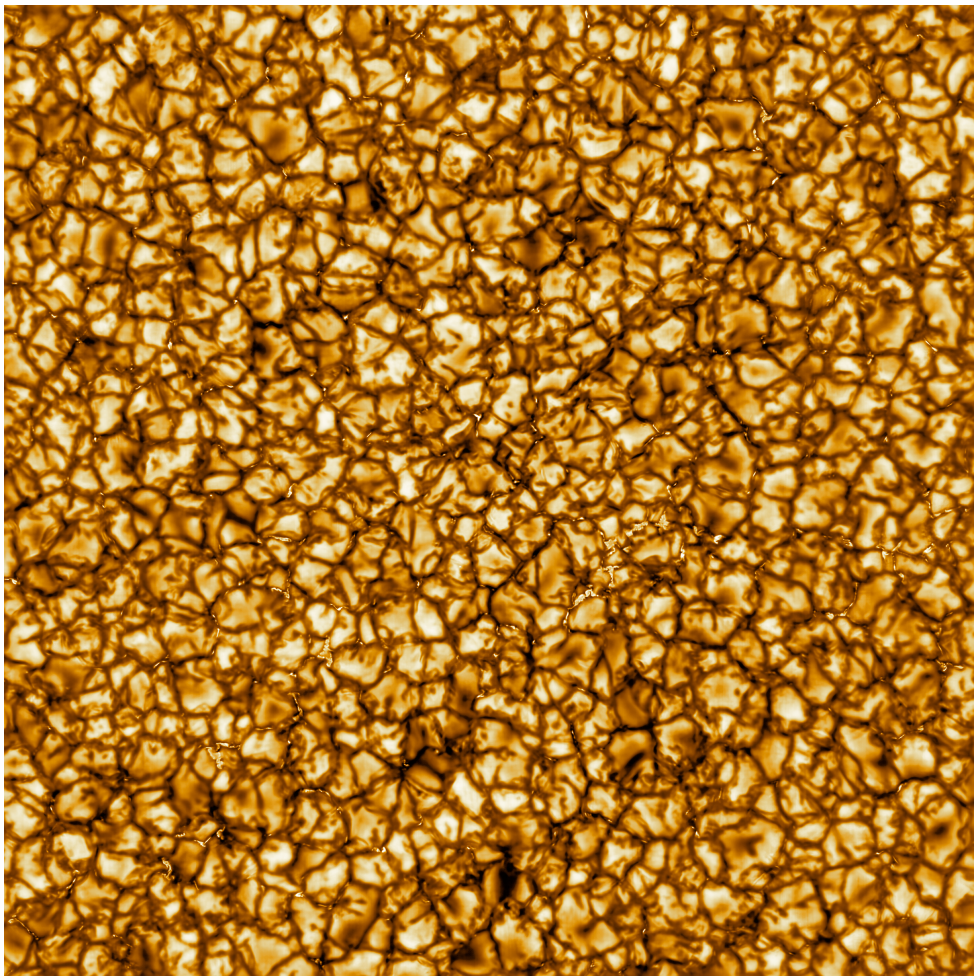

Fig. 1. First light image of the Daniel K. Inouye Solar Telescope (DKIST) on the solar convection. Credits: National Solar Observatory (NSO), National Science Foundation (NSF), Association of Universities for Research in Astronomy (AURA).

the radiation of the free-streaming photons of the upper layers. This high complexity makes difficult the description of the phenomenon and requires a more detailed description and modeling, that deserves further observational and numerical studies.

Fig. 1 shows the highest spatial resolution image of solar convection available at present recently acquired during the first light of the Daniel K. Inouye Solar Telescope (DKIST) (Keil et al., 2009; Woeger, 2016; Rast, 2015; Tritschler et al., 2015).

There are several spectropolarimetric observations of the solar convection and its interaction with the magnetic fields (Berrilli et al., 2001, 2002; Del Moro, 2004; Wilken et al., 1997; Puschmann et al., 2005). The shapes, widths and shift of the solar photospheric spectral lines bring information about the velocity and temperature of the convective plasma and the correlation between these two physical parameters causes the spectral line asymmetries (Asplund et al., 2000). Usually, the more frequently observed spectral lines to infer the

physical properties of the solar convection are the Fe lines, because they are mainly formed in the stable overshooting layer of the photospheric convection (Landi Degl'Innocenti and Landolfi, 2004a). The dimension of the convective cells (see Fig. 1), called *granules*, is approximately 1 Mm (which is the horizontal scale where the convective motions are driven by the radiative cooling), which corresponds approximately to 1 arcsec. They are hotter and brighter than the surrounding and they are associated to upflow plasma movements. The *intergranular lanes*, instead, are cooler and darker and they host a turbulent downflow movement. The density of the solar convective plasma is between 10^{-5} kg/m^3 and 10^{-3} kg/m^3 for the granules and the intergranular lanes, respectively, and the upflow/downflow velocities therein are between ±2 km/s. The observed convective blue-shift of the spectral lines of unresolved sources is caused by the fact that the upflow granules occupies 2/3 of the solar photospheric area and, instead, the downflow intergranular lanes occupied 1/3 of the area (Löhner-Böttcher et al., 2018). The time scale of the convective cells evolution ranges between 5 and 10 minutes.

The solar convection pattern in the photosphere is altered by the presence of the magnetic fields, which have values between few tenths of Gauss and few kGauss (Nordlund et al., 2009; Stein, 2012; Bellot Rubio and Orozco Suárez, 2019). The magnetic elements in the solar photosphere have lower gas pressure and therefore higher magnetic energy than the surrounding, since the sum of the magnetic and the gas pressure must be constant. Therefore, in these magnetized elements, the plasma beta $\beta = p_{gas}/p_{mag}$ is greater than one (Vögler et al., 2005).

The spectrum of the horizontal displacement of the solar magnetic elements scales as $< (\Delta r)^2 > \propto \tau^{\gamma}$, where Δr is the distance between two magnetic elements and τ is the time since the first detection. This epctrum has been evaluated in several works (Giannattasio et al., 2013, 2014a,b, 2018, 2019) and it shows a diffusive exponent γ between 1.20 and 1.55, which is characteristic of the super-diffusive dynamic regime. This result provides a strong evidence that those magnetic elements are transported by the convective motions.

Some magnetic flux tubes, which are located in the intergranular lanes, are called *magnetic bright point* (MBPs, see Fig. 1), and they appear brighter with respect to the surrounding because they are emptied of plasma and their radiation comes from deeper and hotter layers. The MBPs are customarily observed in the G-band at 430 nm of the solar spectrum and they emerge continuously in the solar photosphere with both magnetic polarities, producing phenomena of coalescence, fragmentation and cancellation (Viticchié et al., 2010; Viticchiè et al., 2011; Viticchié, 2012; Guglielmino et al., 2012; Romano et al., 2012; Stangalini et al., 2009; Sánchez Almeida et al., 2010; Martínez González and Bellot Rubio, 2009).

These physical phenomena related to the solar magneto-convection are nowadays observed and studied with top level spectropolarimetric instrumentation based on imaging interferometry or slit spectroscopy. The spatial resolution reached by solar spectropolarimetric observations, given by the 1 m aperture of the current solar telescopes, has been largely exploited; therefore our spectropolarimetric instruments are at their limit of spatial resolution to investigate the finer details of the solar convection. In addition, they suffer from not enough high polarimetric sensitivity. This is the reason because there is a urgent need to built large diameter solar telescope up to 4 m of aperture, such as the recently opened DKIST (Keil et al., 2009; Woeger, 2016; Rast, 2015; Tritschler et al., 2015) and the planned European Solar Telescope (Collados, 2008; Collados et al., 2010a,b; Zuccarello and EST Team, 2012). The four time larger diameter of new-generation solar telescopes will allow us to capture more photons, therefore increasing the spectral resolution and the polarimetric sensitivity, and to reach an angular resolution of 0.04″ (corresponding to 30 km on the solar photosphere) with the use of Adaptive Optics (AO) and Multi-Conjugates Adaptive Optics (MCAO).

Radiative magnetohydrodinamic (MHD) numerical simulations are able to reproduce with high fidelity the granulation pattern

including the interaction with the magnetic fields (Vögler et al., 2005; Gudiksen et al., 2011) and other observed phenomena, such as the reduction of the granules dimension and the appearance of the MBPs in the intergranular lanes. But those simulations still can not predict the evolution of magnetic structures and describe sufficiently all the phenomena that are observed with realistic values of the involved physical quantities (Nordlund et al., 2009; Stein, 2012). Numerical simulations are not only used to explain the physical processes or to validate the observational hypotheses, but also to formulate predictions about observations. Recent simulations (Calvo et al., 2016) show that some brightness enhancements, interpreted as MBPs, should be instead of convective origin because the swirling motion in small regions with lower density could produce a depression due to the centrifugal force, causing and enhancement of the radiation, which comes from an hotter and deeper layer. This phenomenon has not yet been observed due to the spatial resolution limit of present solar telescopes.
The aim of this work, which reports on the main results of my PhD thesis, is to provide a better characterization of the solar turbulent magneto-convection using two complementary approaches: data analysis and instrument design and development.

2. Spectropolarimetric Analysis of a Solar Convection dataset

2.1. Solar Spectropolarimetry and Analysis Methods

Solar spectropolarimetry is a powerful tool to investigate physical processes occurring in the solar atmosphere. The different states of polarization of the light at different wavelengths have in fact encoded the information about the dynamical and the thermodynamical states of the solar plasma and the interacting magnetic fields. The propagation of an electromagnetic radiation through a stellar atmosphere is a non-linear, complex, three-dimensional and time dependent problem and it involves the physical properties of the whole atmosphere (Landi Degl'Innocenti and Landolfi, 2004b; Landi Degl'Innocenti, 2004; Viavattene et al., 2019c). Following the notation of Landi Degl'Innocenti and Landi Degl'Innocenti (1985), the radiative transfer equation (RTE) describes how the radiation propagates through the stellar/solar atmosphere:

$$\frac{d\mathbf{I}}{d\tau} = \mathbf{K}(\mathbf{I} - \mathbf{S}) \tag{1}$$

where $\mathbf{I} = (I, Q, U, V)^T$ is the Stokes vector (which describes the polarization state of the light through the 4 Stokes profiles I, Q, U and V), τ is the optical depth at the transition wavelength, $\mathbf{K}$ is the propagation matrix (which describes the phenomena of absorption, dichroism and dispersion) and $\mathbf{S}$ is the source function vector (which is the Planck function in Local Thermodynamic Equilibrium (LTE)). The elements of the $\mathbf{K}$ matrix depend on the magnetic field intensity B, inclination θ and azimuth ϕ, the line-to-continuum absorption coefficient η_0, and on the absorption and dispersion profiles, which depend in their turn on the Doppler width (broadening due to the thermal motion), the Voigt and the Faraday-Voigt functions. These two functions are directly connected with the damping parameter (which accounts for the collisional effect) and the Doppler velocity of the moving plasma. In this regard, the observation of the different polarization states of the light at different wavelength gives us information about the physical processes involved in the observed phenomena.
In this work, two methods are used to analyze solar spectropolarimetric data: the Center of Gravity Method and the inversion techniques.
The Center of Gravity (CoG) Method (Semel, 1967; Rees and Semel, 1979; Landi Degl'Innocenti and Landolfi, 2004a) is one of the simplest methods used to solve the RTE and to obtain the values of magnetic field and the velocity along the Line-of-Sight (LoS). When the magnetic field is below a few hundreds of Gauss, it is proportional to the amplitude of the Stokes V lobes, and the weak field approximation is valid, so that

$\bar{g}\frac{\Delta\lambda_B}{\Delta\lambda_D} << 1$, where $\bar{g}$ is the effective Landé factor of the observed spectral line, $\Delta\lambda_B$ is the Zeeman splitting caused by the magnetic field and $\Delta\lambda_D$ is the Doppler width of the line. Under this assumption, the LoS magnetic field and LoS velocity can be determined using the following equations:

$$B_{LoS} = B\cos\gamma = \frac{1.071\times10^9}{\bar{g}\lambda_0^2}(\lambda_+ - \lambda_-) \quad (2)$$

$$v_{LoS} = \frac{\int I(\lambda)\lambda\, d\lambda}{\int I(\lambda) d\lambda} \quad (3)$$

where:

$$\lambda_\pm = \frac{\int [I_c - I_\pm(\lambda)]\,\lambda\, d\lambda}{\int [I_c - I_\pm(\lambda)]\, d\lambda} \quad (4)$$

$$I_\pm(\lambda) = \frac{1}{2}\,[I(\lambda) \pm V(\lambda)] \quad (5)$$

and λ is the wavelength. The CoG Method requires short computational time and it is usually used for a rapid estimation of the LoS magnetic field and LoS velocity.

The weak field approximation and the CoG Method can only reproduce a simple atmosphere; nature is always more complex than this. Asymmetric Stokes profiles are often observed in solar spectropolarimetric datasets and it is necessary to increase the complexity of the atmospheric model to match the observations. Indeed, the physical parameters of the solar atmosphere vary with the geometrical depth, and therefore with the optical depth. A more proper approach to analyze this kind of solar spectropolarimetric datasets is to use the strategy of the inversion (del Toro Iniesta and Ruiz Cobo, 2016). If the physical parameters of the atmosphere are known, we can make a *synthesis* of the emergent Stokes vector using the RTE. But in observational solar physics one of the fundamental goals is to solve the opposite problem, which therefore is that of extract the physical conditions of the atmosphere from the observed Stokes vector, making and *inversion* of the RTE (Ruiz Cobo and del Toro Iniesta, 1992, 1994). Inversion codes like SIR (Stokes Inversion based on Response function) (Ruiz Cobo and del Toro Iniesta, 1992) or NICOLE (Non-LTE Inversion COde using the Lorien Engine) (Socas-Navarro et al., 1998, 2000; Socas-Navarro, 2015; Socas-Navarro et al., 2015), find a numerical solution of the RTE using iterative processes based on the Levenberg-Marquardt algorithm (Levenberg, 1944; Marquardt, 1963), until a best fit between the observed Stokes vector $\mathbf{I}_{obs}(\lambda)$ and the synthetic one $\mathbf{I}_{syn}(\lambda)$ is achieved by minimizing a merit function χ. Therefore, the inversion codes retrieve a stratification of the physical parameters of the solar atmosphere (T, p_e, v_{mic}, B, θ, ϕ, v_{LoS}), which better reproduce the spectral line asymmetries.

2.2. Comparison between Center-of-Gravity Method and spectropolarimetric inversions on a quiet-Sun convection dataset

The spectropolarimetric dataset used in this work was acquired with the Interferometric BIdimensional Spectropolarimeter (IBIS) (Cavallini, 2006) installed at the Dunn Solar Telescope (DST) on 2006 November 21st. IBIS measured the 4 Stokes profiles in the spectral region containing two Fe I spectral lines at 630.15 nm and 630.25 nm and simultaneous and co-spatial broad-band images in the G-band. The Field-of-View (FoV) imaged by IBIS is near the disk center and it is $40'' \times 40''$ (corresponding to 30×30 Mm^2 on the solar photosphere), the spatial resolution is $0.17''$ (corresponding to 120 km on the solar photosphere), the time resolution is 89 seconds (time to perform a complete spectral scan) and the total duration of the dataset is approximately on hour (41 spectral scans). The dataset has been calibrated using the IBIS standard pipeline (Viticchié et al., 2010).

This dataset has been analyzed to characterize the solar convection with two physical parameters: B_{LoS} and v_{LoS}, both determined with CoG Method and NICOLE code. Regarding the CoG analysis, Eq. 2 and Eq. 3 are used to compute the LoS magnetic field intensity and

the LoS velocity, hereafter referred as B_{CoG} and v_{CoG}, pixel by pixel for each spectral scan. The dataset has been also inverted pixel by pixel with NICOLE inversion code retrieving the LoS magnetic field and the LoS velocity, hereafter referred as B_{inv} and v_{inv}. For further details on this analysis, see Viavattene et al. (2018).

Fig. 2 shows the maps of B_{CoG} and B_{inv} of one spectral scan. It can be noticed that, although the analysis has been performed pixel by pixel, both methods retrieve coherent magnetic structures. Fig. 3 shows the Probability Density Functions (PDFs) of B_{CoG} and B_{inv}, computed excluding the pixels with signals lower than three times the noise. The wings of the PDF of B_{CoG} break down at approximately ± 500 G due to the saturation effect of the CoG Mehod for magnetic fields greater than 400 G, since the weak field approximation is not valid anymore. The PDF of B_{inv}, instead, is very peculiar because its central part is not symmetric and two asymmetric bumps at ± 100 G are clearly visible. A possible explanation of these two features is that inversion techniques tend to overestimate the weak magnetic fields: in fact, the two bumps could be generated by the pixel that should have lower values but are redistributed to higher values by the inversions (Viavattene et al., 2018; del Toro Iniesta and Ruiz Cobo, 2016).

Similarly, the maps of v_{CoG} and v_{inv} are reported in Fig. 4. The granulation pattern is clearly visible, with the upflow granules and the downflow intergranular lanes. The PDFs of v_{CoG} and v_{inv} are reported in Fig. 5. Both have the maximum at 0 km/s, but different shapes: the PDF of v_{CoG} is more symmetric because the CoG Method retrieves the physical information "averaged" in the atmospheric layer where the spectral line is mainly formed; the PDF of v_{inv} is asymmetric because the inversion techniques retrieve a stratification of a physical parameter with respect to the optical depth and therefore the values at a given layer ($\log\tau = -1$ for comparison with the CoG Method) are influenced by the value in the neighboring atmospheric layers. The spike at $v_{inv} = -2$ is the effect of those inversions which did not converge to a solution, and the two bumps stand for pixels with high value of downflow velocity associated with high photospheric temperature profiles, which have no physical meaning.

The results of this comparison analysis show that the CoG Method requires less computational time but it is based on more assumption and it retrieves the values of the atmospheric parameters in the "averaged" layer where the spectral line is mainly formed; the inversion technique, instead, requires more computational time, it retrieves a more complete description of the observed phenomenon, since it provides a stratification of the atmospheric parameters, but it has the tendency to overestimate the weak magnetic fields.

2.3. The Solar Convection as a Non-Equilibrium Steady-State system

The physical system of the solar convection presents phenomena related to strong turbulence in the intergranular lanes due to the high Rayleigh number of the upper convection layer and due to the high density stratification, making the Sun the only observable system where to analyze these extreme processes. In fact, the high Rayleigh number of the solar convection ($> 10^{12}$) is not reproducible in laboratory experiments (maximum Rayleigh number ever reached is 10^7) (Niemela et al., 2000).

Linear and non-linear statistical thermodynamics predicts that in systems out of equilibrium there is a spontaneous production of entropy which originates the irreversibility, according to the second law of thermodynamics. In particular, the entropy production rate is the physical parameter used to described the departure from equilibrium of such systems (De Groot and Mazur, 2013). The study of the entropy fluctuations in the granules and in the intergranular lanes, which drive the solar convection, could be of relevant importance to validate this general theory. Thus the Sun becomes a natural laboratory where the physics of turbulent convection with high Rayleigh number can be investigated.

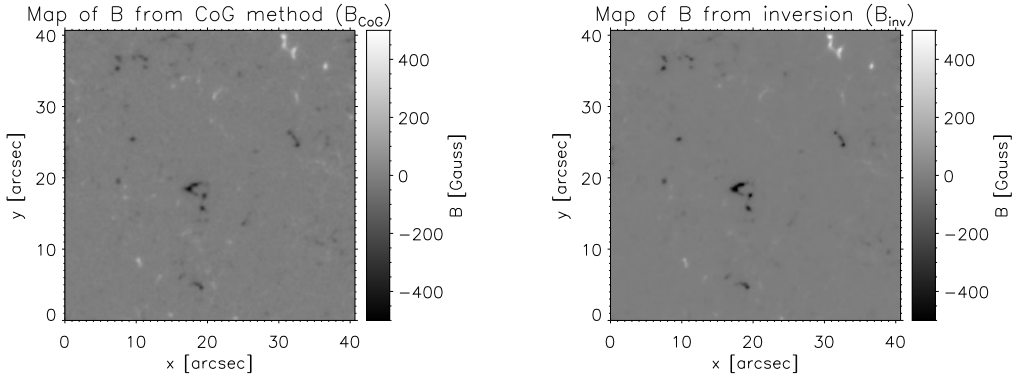

Fig. 2. Left panel: Map of the LoS magnetic field evaluated with the CoG Method. Right panel: Map of the LoS magnetic field evaluated with NICOLE inversions. Figure adapted from Viavattene et al. (2018).

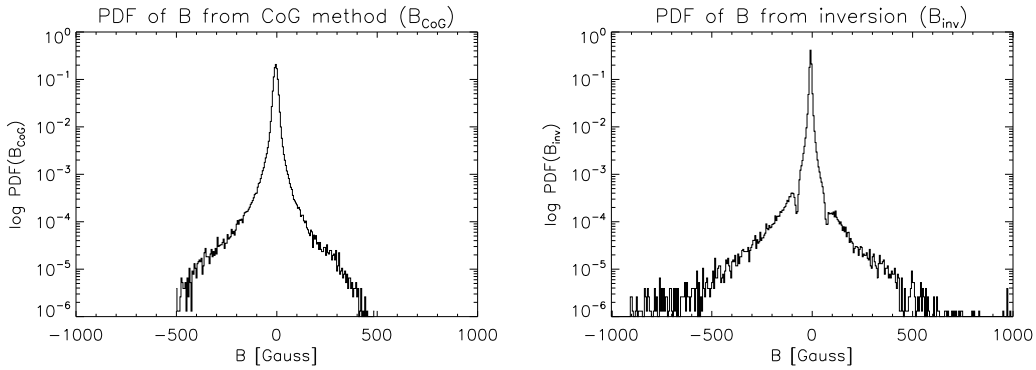

Fig. 3. Left panel: PDF of the LoS magnetic field evaluated with CoG Method. Right panel: PDF of the LoS magnetic field evaluated with NICOLE inversions. Figure adapted from Viavattene et al. (2018).

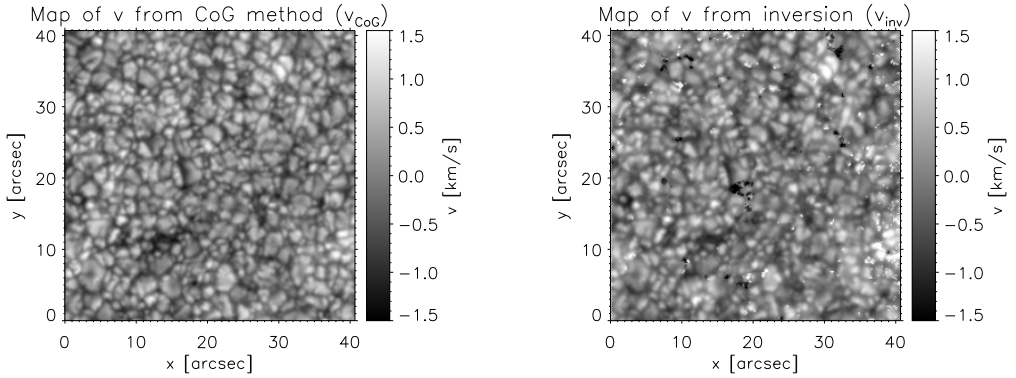

Fig. 4. Left panel: Map of the LoS velocity evaluated with the CoG Method. Right panel: Map of the LoS velocity evaluated with NICOLE inversions.

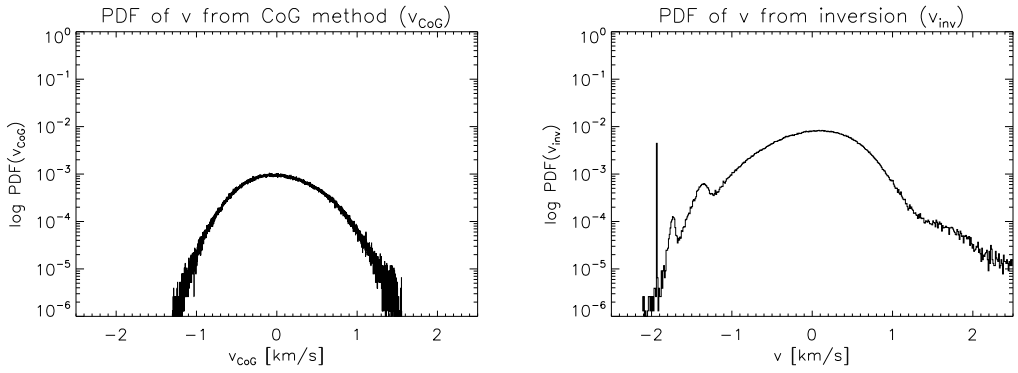

Fig. 5. Left panel: PDF of the LoS velocity evaluated with CoG Method. Right panel: PDF of the LoS velocity evaluated with NICOLE inversions.

In the last decades, several works have been presented to describe the entropy production rate fluctuations in non-equilibrium systems. The Gallavotti-Cohen Fluctuation Relation (GCFR) (Gallavotti and Cohen, 1995) is one of the most important of these and it describes the symmetry features of a dimensionless characterization of the phase space contraction rate p in non-linear and out of equilibrium regime under the time-reversal and chaotic assumption. The GCFR can be expressed as follows:

$$\lim_{\tau\to\infty} \frac{1}{\tau\sigma_+} ln \frac{\pi_\tau(+p)}{\pi_\tau(-p)} = p \tag{6}$$

where $\pi(\pm p)$ is the probability of finding a positive or negative value of the phase space contraction rate and σ_+ is the average phase space contraction rate over an infinite time. In general, the GCFR is also valid for a flux quantity, such as heat, energy, momentum flux, entropy production rate, and so on, since it is related to the statistics of a variable linked to the phase space contraction rate. For the vertical heat flux J, the GCFR can be written as follows:

$$\lim_{\tau\to\infty} \frac{1}{\tau} \ln \frac{\pi(J_\tau = J)}{\pi(-J_\tau = -J)} = \alpha_+ J, \tag{7}$$

where α_+ is a constant. Despite the GCFR was initially inferred for global quantities, it was also proved to be valid in the time averaged quantities $J_\tau(\mathbf{r}) = \frac{1}{\tau}\int_t^{t+\tau} J(\mathbf{r}, t')dt'$ and for local quantities (Gallavotti, 1999; Evans and Searles, 2002). In the asymptotic regime ($\tau \to \infty$), the following linear relation is valid: $\alpha(\tau) \sim \alpha_+\tau$, thus obtaining:

$$\ln \frac{\pi(+J_\tau)}{\pi(-J_\tau)} \sim \alpha_+ \tau J_\tau \tag{8}$$

Although there are some instrumental verification of the validity of the GCFR in different laboratory setups (Ciliberto et al., 2004; Shang et al., 2005), there are no observational verifications of it on a real physical or astrophysical system. In this regard, the dissipative processes of the solar convection, viewed as a Non-Equilibrium Stationary-State (NESS) system, turn into an unequaled laboratory to test the GCFR.

Following Shang et al. (2005), the local vertical heat flux $j_z(\mathbf{r}, t)$, where $\mathbf{r}$ is the vector position and t is the time, can be used as a proxy of the local entropy production rate $\sigma(\mathbf{r}, t)$, since $\sigma(\mathbf{r}, t) \approx V_0 j_z(\mathbf{r}, t)\nabla_z\left(\frac{1}{T}\right)$, where V_0 is the volume in which the local quantities are evaluated and $\nabla_z\left(\frac{1}{T}\right)$ is the vertical gradient of the temperature T. The local vertical heat flux $j_z(\mathbf{r}, t)$ can be computed as follows:

$$j_z(\mathbf{r}, t) \sim v_{LoS}(\mathbf{r}, t)\delta T(\mathbf{r}, t) \tag{9}$$

where $\delta T(\mathbf{r}, t) = T(\mathbf{r}, t) - T_0$, with T_0 the average temperature.

Using the same IBIS/DST spectropolarimetric dataset of the previous section, the temperature maps $T(\mathbf{r}, t)$ have been evaluated using

the Stefan-Boltzmann black body radiation law and the LoS velocity maps $v_{LoS}(\mathbf{r}, t)$ have been evaluated using the CoG Method. For further details on this analysis, see Viavattene et al. (2019a,b). Since we are interested in the solar convection pattern not altered by the presence of magnetic fields, we excluded those pixels with a magnetic field intensity greater than 50 G. A sample of temperature and LoS velocity maps are reported in Fig. 6. An example of a vertical heat flux maps is showed in Fig. 7 (left panel).

To study the statistics of $j_z(\mathbf{r}, t)$ and to test the steady state of the GCFR, a running average of $j_z(\mathbf{r}, t)$ over a time interval τ has been computed using the following relation:

$$J_\tau(\mathbf{r}, t) = \frac{1}{\tau} \int_t^{t+\tau} j_z(\mathbf{r}, t')dt'. \quad (10)$$

The Probability Density Functions (PDFs) evaluated with the Kernel Method (Kaiser and Schreiber, 2002) for some values of $J_\tau(\mathbf{r}, t)$ are reported in Fig. 7 (right panel). The PDFs shrink when τ increases and the most probable value tends to a non-zero value for high values of τ. The shapes of the PDFs are clearly non-Gaussian and asymmetric and this confirms that the solar convection is a non-equilibrium process. In particular, their lepto-kurtotic shapes are characteristic of turbulent processes.

In Fig. 8 (left panel), the logarithmic ratio from Eq. 8 has been reported for the same value of the PDFs of $J_\tau(\mathbf{r}, t)$ showed in Fig. 7 (right panel). The linear fits are overplotted with dashed lines. It can be noticed that the slopes of the linear fits increase when τ increases. In Fig. 8 (right panel), the plot of the $\alpha(\tau)$ parameter is shown. The linear fit is performed for $\tau > 900$ s. It can be clearly noticed that there is a good linear behaviour between α and τ, especially for $\tau \sim 600 \div 800$ s, which is the typical lifetime of the convection cells (Berrilli et al., 2002). In addition, by rescaling α_+ with the asymptotic values of $J_\infty \sim 20$ km K s^{-1}, a typical dissipation time scale τ_{diss} of the order of $100 \div 120$ s is obtained, which is in the same range of the typical velocity decorrelation time (Berrilli et al., 2002) and in the same range of the thermal adjustment time, which is the time for the release of the excess of the thermal energy. These evidences reinforce considerably the GCFR validity test on the solar convection. For other details, see Viavattene et al. (2020b).

To conclude, we investigated the validity of the GCFR on the solar turbulent convection. The PDFs of the local vertical heat flux are asymmetric and with a non-zero asymptotic value, confirming that the solar convection produces entropy spontaneously, as expected from a NESS system. The obtained results are the first verification of the GCFR in a real astrophysical system (Viavattene et al., 2020b).

3. Solar Physics instrumentation development

Modern Solar Physics requires top level technologies for its telescopes and their suite of spectropolarimetric instruments to acquire data with high spatial, spectral and temporal resolution in order to study the magnetic, dynamic and thermodynamic properties of the solar atmosphere. Solar telescopes are usually build in a 25-30 m tower or on a platform inside a lake to limit the effect of the diurnal seeing caused by the warming of the surrounding soil. The telescope tubes are evacuated or fully opened with a truss structure in order to reduce the seeing caused by the warming of the optical path. The use AO or MCAO systems is in any case mandatory to minimize the daytime seeing and to improve the effective angular resolution up to the diffraction limit of the telescope. The first limiting parameter is the angular resolution $\alpha_{min} = 1.22\frac{\lambda}{D}$ given by the telescope aperture D at the observed wavelength λ. The second enabling technology is the capability of an instrument to distinguish a spectral feature, which is usually expressed with the spectral resolving power $\mathcal{RP} = \frac{\lambda}{\Delta\lambda}$. The Sun is a spatially extended source, therefore solar physicists want to record 3D information (x-position and y-position on the Sun, and the wavelength). Unfortunately, nowadays we have only 2D detectors, and there are two different ap-

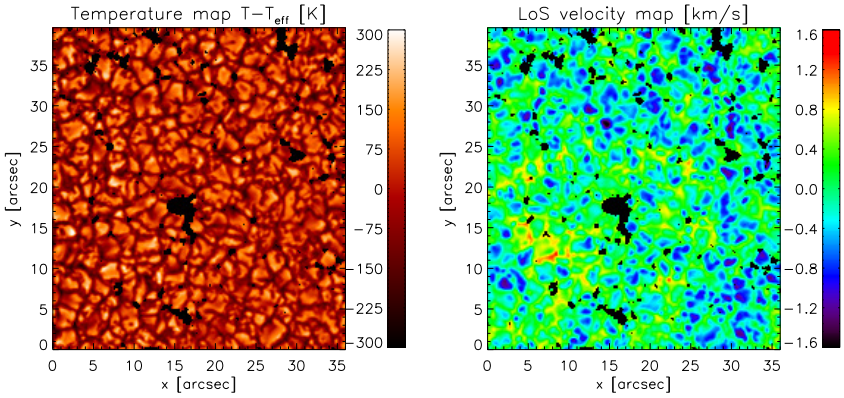

Fig. 6. Left panel: a sample of a temperature map evaluated using the Stefan-Boltzmann black body radiation law. Right panel: LoS velocity map evaluated using the CoG method. Black pixels mask those regions excluded from our analysis because they have magnetic field intensity greater than 50 Gauss. Figures adapted from Viavattene et al. (2019a).

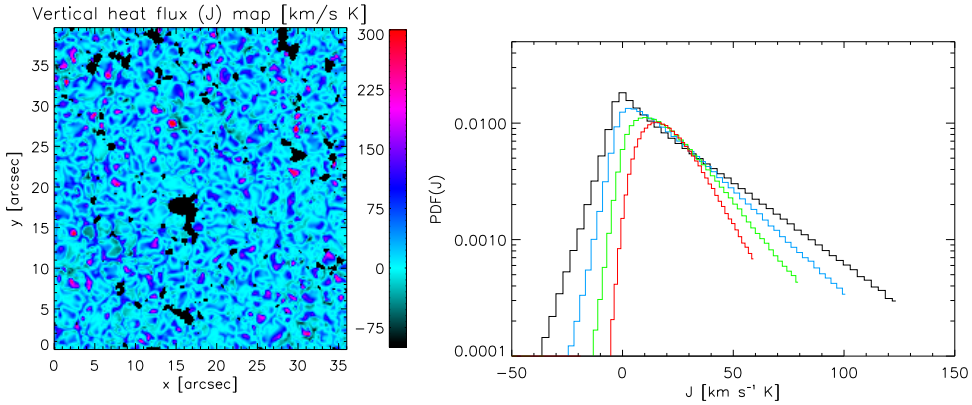

Fig. 7. Left panel: sample vertical heat flux map. As Fig. 6, black pixels mask those regions excluded from the analysis. Right panel: PDFs of the J_τ evaluated with the Kernel Method: black is for J_2, light blue for J_4, green for J_8 and red for J_{16}. Figures adapted from Viavattene et al. (2019a) and from Viavattene et al. (2020b).

proaches to recover a 3D information on them: to select a slice of the image and to disperse the various components of the light (with a prism or grating) and then moving the slice along the image (slit-spectroscopy), or to filter in wavelength the incoming light of the image and then changing the spectral position of the filter (spectro-imaging). Between these two techniques, the second one is to be preferred since the instruments based on Fabry-Perot Interferometer (FPI) are more efficient with respect to the ones based on grating spectrometer, although they reach a lower spectral resolution. A FPI uses the multiple-beam interferometry inside its optical cavity made by two partially reflecting mirrors to produce a spectral comb transparency profile. The spectral comb can be shifted in wavelength

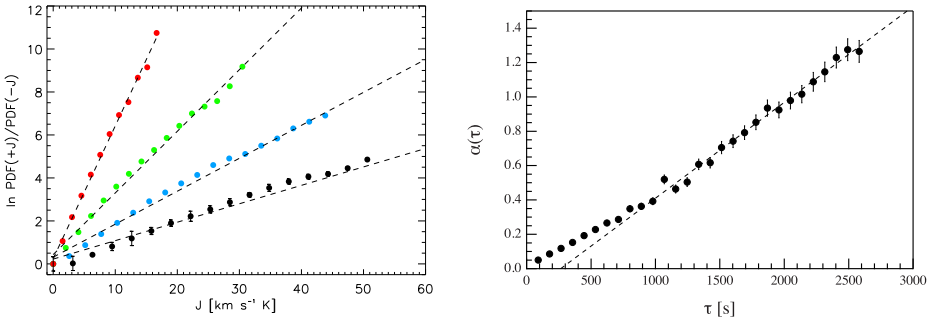

Fig. 8. Left panel: logarithmic ratios averaged with τ evaluated using Eq. 8. Same colours of Fig. 7. The dashed lines are the linear fits performed in the linear parts of the plots. Right panel: $\alpha(\tau)$ parameter from Eq. 6. The dashed line is the linear fit for $\tau > 900$ s. Figures adapted from Viavattene et al. (2020b).

by varying the spacing of the optical cavity. Combining the FPI with a suitable *prefilter* which selects one of the peaks of the spectral comb, an FPI-based instrument can be used to perform spectro-imaging. In addition, a largely used approach in Solar Physics is to use two or more FPIs in tandem in order to obtain higher spectral resolution.

3.1. Fabry-Perot Prototype for the GREST Project

The fine control of the parallelism and the positioning of the two plates of an FPI is of fundamental importance to obtain the correct spectral sampling. In this section, the design and development of a Capacitance Stabilized Etalon (CSE) controlled with one of the first digital controllers is reported. A CSE is an FPI whose spacing is driven by piezo-electric (PZT) actuator and controlled by capacitive sensors. The development of digital controllers for CSEs is one of the most importart technological challenging for large-diameter FPI, which will be largely used for 4-m class solar telescopes like EST or DKIST.

The GREST FPI 50 and the ADS100 controller are two prototypes developed by the Solar Physics Group of the University of Tor Vergata and the ADS International company of Lecco (Milan, Italy) in the framework the GREST WP3 project (`https://est-east.eu/index.php/grest`). The FPI 50 is a CSE with an optical cavity of 50 mm in diameter (λ/20 of optical quality) with three PZTs (0-150 V DC) in a 120° geometry and monitored by five capacitive sensors coupled in capacitive bridge circuit. The two plates have a spacing of approximately 1 mm and they are mounted in an housing that allows to regulate their mutual tilt and spacing using three micrometers, which insist on the three PZTs. The six 22 pF capacitive sensors are made by gold plated mirrors at a working distance of 50 μm, which can be set using other micrometers. Two capacitive sensors are used to monitor the tilt along the x-axis, other two for the tilt along the y-axis and one coupled with an external reference capacitive sensor (for the capacity drift due to the air properties variation) is used to monitor the plate distance.

The ADS100 has been developed by ADS International in order to control the GREST FP 50 prototype and it will replace the old analogical controllers for CSE. It is a milestone for the control of the closed loop stability with the ability of digital filtering of the signal during the spectral line scan. The ADS100 is made by several components: the digital-to-analog converter for the PZTs, the high voltage amplifier, the capacitive sensors interface and a PIC32 microprocessor. The

whole system is controlled by a Raspberry PI. Programs developed in C and Python 2.7 are dedicated to the calibration of the capacitive sensors response after a PZT stroke, to maintain the plate parallelism in closed loop with a frequency up to 40 Hz and to perform a spectral scans varying the optical cavity spacing. The GREST FPI 50 connected with the ADS100 controller is shown in Fig. 9.

The electronic stability tests have been performed using a climatic chamber in the ADS International Laboratory with a temperature of 20±1°C and a humidity of 65±1%. The standard deviation of the noise of the ADS100 connected with NP0 capacitance (high tolerance and stability in temperature) is of the order of 0.15÷0.38 mV. Instead, the standard deviation of the noise of the ADS100 connected with the GREST FPI 50 prototype was 0.20÷0.40 mV.

The optical tests and the spectral characterization of the GREST FPI 50 have been performed in the Solar Physics Laboratory of the University of Rome Tor Vergata placing the FPI alternatively in collimated beams produced by a green laser (532 nm) and a Sodium lamp using suitable lenses. Using the laser beam, the plate parallelism has been performed until only two interference fringes are observed in afocal configuration, obtaining a tilt of the two plates of the order of 200 nm. Repeating the test with the GREST FPI 50 and the ADS100 controller we obtained a noise of 0.25 mV. This value corresponds to a cavity distance noise of 7.6 nm and to a spectral noise of 5.0 pm. Performing a spectral scan using the Sodium lamp, we obtained a spectral sampling of 7.2 pm.

The results obtained during the tests are very promising and satisfying. The noise measured with the GREST FPI 50 is at the requested level, considering the mechanical limitations of the prototype. The ADS100 is therefore able to control a CSE in closed loop up to 40 Hz. Currently, a new version of the the ADS100 with improved performances is under development.

3.2. Feasibility Study of a Narrow-Band Imager based on Large-Diameter Fabry-Perots and Off-Axis Parabolic Mirrors

The design of a FPI-based narrow band imager for 4-m class solar telescopes presents several constraints. The requested spectral resolution greater than 300.000 and a FoV greater than 90″ requires the use of large optical elements, and this implies large optical path. In particular, with these requirements, the conservation of the optical étendue imposes the use of FPI with a diameter of 200-250 mm.

In this section, a feasibility study of an optical scheme proposed by Greco and Cavallini (Greco and Cavallini, 2013) is presented with the aim of reducing the encumbrances of the instruments maintaining the original high optical and spectral performances. The conceptual idea of Greco and Cavallini was proposed for DKIST and it consists on a narrow band imager based on large diameter (20 cm) FPIs and off-axis parabolic mirrors with top level instrumental performances: $\mathcal{RP} > 300.000$, FoV> 90″, high angular resolution ~0.05″, exposure time < 10ms to freeze the Earth's atmospheric seeing, wavelength range of 850-1650 nm and instrumental polarization <0.5%. The 2D-plano optical design proposed by Greco and Cavallini uses two FPIs of 200 mm of aperture and interference prefilters of 70 mm of aperture (the best achievable with modern coatings) all placed in pupil planes. The beam is focused and collimated using large diameter off-axis parabolic mirrors coupled to each others in order to cancel their polarimetric contributions to the signal. For details, see Greco and Cavallini (2013).

Several 3D optical configurations have been exploited in order to reduce the encumbrances of the 2D design of Greco and Cavallini. The frontal and the lateral views of the most functional configuration have been reported in Fig. 10. With respect to the initial conceptual idea of Greco and Cavallini, some changes on the positions of the optical elements are proposed, but no changes on their optical properties (optical distances, curvature radii, and so on). After the focus of M1, FPI1 is

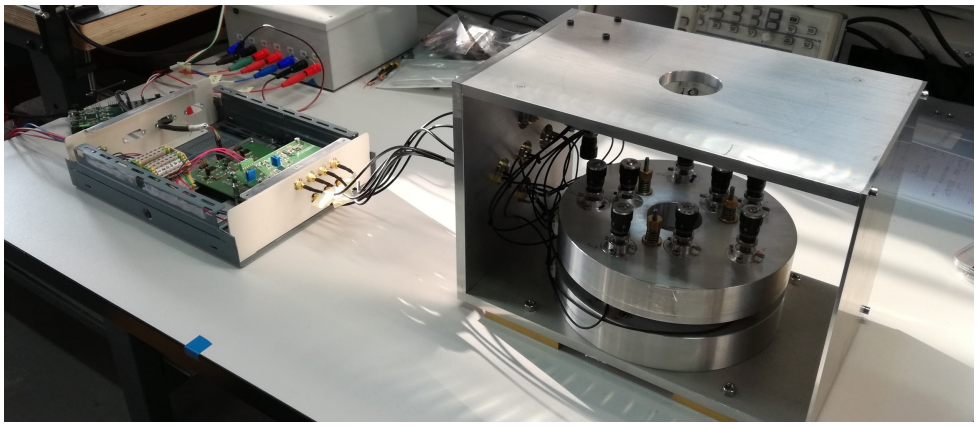

Fig. 9. The GREST FPI 50 connected to the ADS100 controller.

placed in the pupil between mirrors M2 and M3, the prefilter is placed in the pupil between M4 and M5, FPI2 in the pupil between M6 and M7, and finally, after M8 the focal plane image on the CCD detector is made by the achromatic doublet D. The new 3D optical design forecasts that mirrors M1, M4-M5 and M8 are moved up and different sectors of the off-axis parabolic mirrors are illuminated by the beam. With this solution the encumbrance of the instrument is significantly reduced and the polarization-free requirements is maintained: in fact, as showed in Fig. 10, a 90-degrees complementary angles geometry has been chosen between the coupled mirrors M1-M2, M3-M4, M5-M6 and M7-M8 in such a way that the polarization introduced by one mirror is compensated by the coupled mirror. Analyzing the spot diagrams, the instrument is still diffraction limited since the image spots are inside the Airy disk for the whole FoV of 90″.

The stringent mounting tolerances (less that 0.05) mm are very difficult to achieve with off-axis parabolic mirrors in order to avoid the large astigmatism and coma introduced by this kind of optical surfaces. Currently, there are several possible ways under investigation to solve this issue on mounting tolerances: 1) to use off-axis parabolic mirrors with longer focal lengths, which are easier to manufacture and less critical to be aligned; 2) to use off-axis parabolic mirrors with less off-axis distance in order to reduce the astigmatism and the coma; 3) to use off-axis Maksutov cameras (made by spherical surfaces and corrective meniscus lens), since they are less sensitive to the collimation and they are free from astigmatism.

3.3. Optical Design and Realization of a Telescope based on Magneto-Optical Filters

To acquire complementary data to support the high-resolution observations, full-disk solar telescopes are needed (FoV>32 arcmin). This kind of solar telescopes are usually used to monitor the large-scale solar activity and the active regions, to study the large scale convection pattern of the solar photosphere and for Space Weather applications. The FPIs can not be used easily for high spectral resolution full-disk observations due to the large angle subtended by the solar disk, which causes a worsening of the FPIs' effective finesse. For this reason, Magneto-Optical Filter (MOF) based telescopes are to be preferred. The optical design of such telescopes is quite critical due to the aberration control on the final focal plane image over the entire FoV. In this section, a short description of the Tor vergata Synoptic Solar Telescope (TSST) is presented.

The TSST (Calchetti et al., 2020; Viavattene

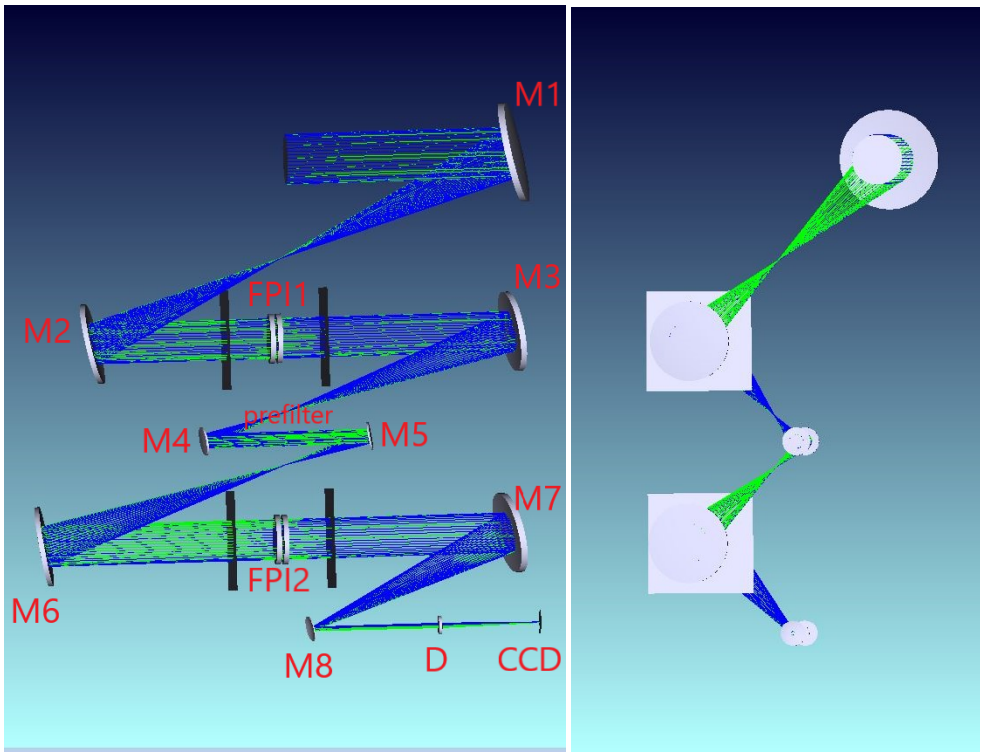

Fig. 10. Frontal view (left panel) and lateral view (right panel) of the new proposed version of the optical scheme for the narrow band imager based on large diameter FPIs and off-axis parabolic mirrors. The dummy square optical surfaces stands for the thermostated box for the FPIs.

et al., 2020a; Forte et al., 2020; Giovannelli et al., 2020) is a double channel solar telescope realized in the Solar Physical Laboratory of the University of Rome Tor Vergata for Space Weather studies. The Hα channel is realized with a Daystar SR-127 telescope which uses an etalon to select the Hα spectral line and it uses a dedicated focal reducer to obtain a full-disk image of the Sun. The MOF-based channel has been entirely designed with Zemax software and it selects the right and left polarized light of the two blue and red wings of the Potassium K D1 spectral line at 769.9 nm exploiting the Macaluso-Corbino effect (Macaluso and Corbino, 1898; Macaluso et al., 1899b,a).

A MOF is a filter based on resonant scattering and it consists on a cylindrical cell filled with a vapour of an alkaline metal placed inside a strong longitudinal magnetic field and between two crossed linear polarizers (Cacciani et al., 1990; Cacciani and Moretti, 1994; Cimino et al., 1968). Thanks to the Zeeman effect, which causes the splitting of the spectral line, and to the Macaluso-Corbino effect, the transmission profile of a MOF is characterized by two peaks placed on the wings of the spectral line. A MOF-based solar telescope can be used to obtain dopplergrams (D) and magnetograms (M) of the entire solar disk by measuring both polarization states (+ and −) in the red (R) and (B) wings of the spectral line using the following relations:

$$D = \frac{R^+ - B^+}{R^+ + B^+} + \frac{R^- - B^-}{R^- + B^-} \tag{11}$$

$$M = \frac{R^+ - B^+}{R^+ + B^+} - \frac{R^- - B^-}{R^- + B^-} \tag{12}$$

The two peaks of the Macaluso-Corbino effect can be separated using a second cell

(called Wing Selector (WS)) filled with the same vapour and with a magnetic field twice that of the MOF cell and using quarter-wave plates (QWPs) and half-wave plates (HWPs). In particular, the MOF channel of the TSST uses the same modulation scheme of the VAMOS (Velocity And Magnetic Observations of the Sun) telescope (Oliviero et al., 1998a,b; Severino et al., 2001; Oliviero et al., 2002): a QWP and a rotating HWP select the polarization state of the solar light, the MOF cell between the two crossed linear polarizers creates the passband with the two spectral peaks, a rotating HWP a QWP and the WS select the blue or the red wing of the passband. For details, see Calchetti et al. (2020); Viavattene et al. (2020a).

The optical scheme of the MOF channel of the TSST as been designed using the Zemax software, as described in Viavattene et al. (2020a). The optical scheme has been implemented following several requirements: 1) entrance pupil diameter of 80 mm in order to have an angular resolution of $2''$; 2) large FoV for full-disk imaging; 3) collimated beam inside the MOF and WS cells to avoid the internal vapour seeing; 4) corrective lens to have an aberration-free focal plane image; 5) and compact scheme to reduce the encumbrances and weights to mount it over a Sky-Watcher EQ8 mount together with the Hα telescope. Among the several studied optical scheme, the adapted final solutions uses two 45° folding mirrors to reduce the total length of the instrument. The optical layout basically consists in a double-Keplerian telescope with an imaging lens and corrective lenses. Some rejection filters are placed between the 80mm objective lens L1 and L2. The interference filter (IF), the QWP, the HWP and the MOF section are placed in the collimated beam between L2 and L3. The HWP, the QWP and the WS are placed in the collimated beam between L4 and L5. Finally the corrective lenses (CL) eliminate all the aberrations (especially the distortion and the field curvature) and form a diffraction limited final focal plane image. For details on the optical schem, see (Viavattene et al., 2020a).

The spectral characterization of the instrument has been performed using a tunable laser at the Observatory of Capodimonte (INAF) in Naples. The magnetic field and the temperature of the MOF cell have been calibrated in order to ensure the proper operation of the filter, namely the two Macaluso-Corbino peaks must be formed properly without transmission between them (temperature tuning) and they must have a distance of 0.02nm (magnetic tuning). The magnetic field and the temperature of the WS cell have been calibrated in such a way that the WS passband must match the MOF peaks in order to select one of them alternatively according to the modulation scheme. For details on the spectral calibration, see Calchetti et al. (2020).

At the present time, the TSST is in assembly and test phase: all the optical components have been mountend and correctly aligned and the first light of the instrument was in May 2020; the mechanical case and its temperature control is in design phase. Future plans foresee the installation of the TSST in a remote dome in one of the Observatory of the Canary Islands, probably at Roque de los Muchachos in La Palma. The TSST will form a network of full-disk solar telescopes together with VAMOS and MOTH (Magneto Optical filters at Two Heights) telescopes, which will be used to retrieve magnetograms and dopplergrams with high temporal cadence for Space Weather applications.

4. Conclusion and Future Perspectives

In this work, some aspects on the observation and characterization of the solar turbulent convection have been presented, which have been addressed through spectropolarimetric data analysis and instrument design and development.

Regarding the data analysis part, an high resolution IBIS/DST spectropolarimetric dataset has been used for a comparison analysis between the Center-of-Gravity Method and the inversion techniques, showing that inversion techniques tend to overestimate weak magnetic fields. The same dataset has been used

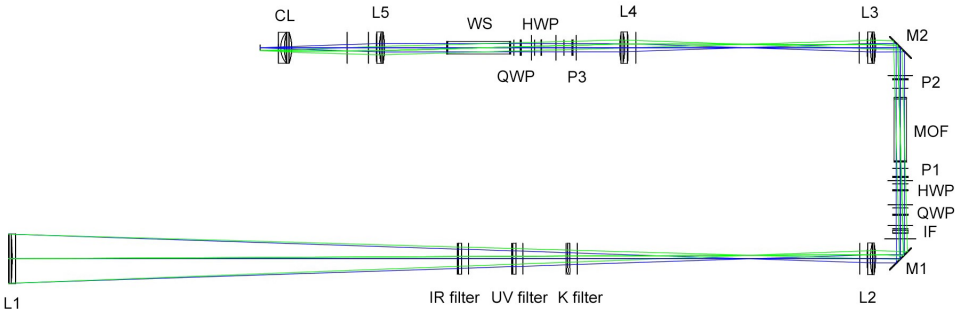

Fig. 11. Optical scheme of the Magneto-Optical Filter (MOF) channel of the Tor vergata Synoptic Solar Telescope (TSST). Figure from (Viavattene et al., 2020a).

to test the validity of the Gallovotti-Cohen fluctuation relation on the solar convection, obtaining strong evidence for its validity and confirming that the solar convection can be modeled as a NESS system with a positive production of entropy.

For the instrumental part, three different projects have been presented. A Fabry-Perot interferometer prototype controlled by the ADS100 digital controller has been design and developed in collaboration with ADS International Company of Lecco, obtaining very promising results on the electronical noise and stability of the system, opening a way to the next generation instruments for large diameter solar telescopes. Following the trail of next generation instruments based on Fabry-Perot interferometers, a feasibility study for a narrow band imager based on large diameter interferometers and off-axis parabolic mirrors has been performed; a new 3D configuration has been implemented following the conceptual idea of Greco and Cavallini and its instrumental tolerances has been analyzed. Finally, the entire optical scheme of a Magneto-Optical Filter based telescope has been realized for the Tor vergata Synoptic Solar Telescope (TSST), a telescope that will be primarily used for Space Weather applications but it could be also used to study the large scale patterns of the solar convection.

Concluding, this work shows how the study of Solar Physics requires a multidisciplinary approach, going from the radiative transfer to the non-equilibrium statistical thermodynamics. Indeed, the high complexity of the solar magneto-convection needs top-level high resolution instrumentation and large diameter solar telescopes (like DKIST or EST) to produce high resolution spectro-polarimetric data, which are analyzed with several techniques and which are compared with models obtained via numerical simulations.

Acknowledgements. I would like to thank my PhD tutor Dr. Dario Del Moro and my PhD cotutors Dr. Giuseppe Consolini and Dr. Luca Giovannelli for guiding me during the three years of my PhD and for the scientific and research opportunities that they gave me. I thank also the head of the "Tor Vergata" Solar Physics group Prof. Francesco Berrilli for his scientific guidance. I would like to thank the Organizers and the Committee of the Tacchini Award for giving me the Special Mention and the opportunity to publish this work with the scientific and instrumental results of my PhD.

References

Asplund, M., Nordlund, Å., Trampedach, R., Allende Prieto, C., and Stein, R. F. (2000). Line formation in solar granulation. I. Fe line shapes, shifts and asymmetries. *Astronomy and Astrophysics*, 359:729–742.

Bellot Rubio, L. and Orozco Suárez, D. (2019). Quiet Sun magnetic fields: an observational view. *Living Reviews in Solar Physics*, 16(1):1.

Berrilli, F., Consolini, G., Florio, A., and Pietropaolo, E. (2001). Solar granulation: properties of velocity fields from THEMIS-IPM observations. *Memorie della Societa Astronomica Italiana*, 72:669–672.

Berrilli, F., Consolini, G., Pietropaolo, E., Caccin, B., Penza, V., and Lepreti, F. (2002). 2-D multiline spectroscopy of the solar photosphere. *A&A*, 381:253–264.

Cacciani, A. and Moretti, P.-F. (1994). Magneto-optical filter: concept and applications in astronomy. In Crawford, D. L. and Craine, E. R., editors, *Proc. SPIE*, volume 2198 of *Society of Photo-Optical Instrumentation Engineers (SPIE) Conference Series*, pages 219–228.

Cacciani, A., Ricci, D., Rosati, P., Rhodes, E. J., Smith, E., Tomczyk, S., and Ulrich, R. K. (1990). Solar magnetic fields measurements with a magneto-optical filter. *Nuovo Cimento C Geophysics Space Physics C*, 13:125–130.

Calchetti, D., Viavattene, G., Berrilli, F., Del Moro, D., Giovannelli, L., and Oliviero, M. (2020). Tor vergata Synoptic Solar Telescope: preliminary optical design and spectral characterization. In *Journal of Physics Conference Series*, volume 1548 of *Journal of Physics Conference Series*, page 012005.

Calvo, F., Steiner, O., and Freytag, B. (2016). Non-magnetic photospheric bright points in 3D simulations of the solar atmosphere. *A&A*, 596:A43.

Cavallini, F. (2006). IBIS: A New Post-Focus Instrument for Solar Imaging Spectroscopy. *Sol. Phys.*, 236:415–439.

Ching, E. S. C. (2014). Statistic and scaling in turbulent rayleigh-bénard convection.

Ciliberto, S., Garnier, N., Hernandez, S., Lacpatia, C., Pinton, J.-F., and Ruiz Chavarria, G. (2004). Experimental test of the Gallavotti-Cohen fluctuation theorem in turbulent flows. *Physica A Statistical Mechanics and its Applications*, 340:240–250.

Cimino, M., Cacciani, A., and Sopranzi, N. (1968). An Instrument to measure Solar Magnetic Fields by an Atomic-Beam Method. *Sol. Phys.*, 3(4):618–622.

Collados, M. (2008). European Solar Telescope (EST): project status. In *Ground-based and Airborne Telescopes II*, volume 7012 of *Proc. SPIE*, page 70120J.

Collados, M., Bettonvil, F., Cavaller, L., Ermolli, I., Gelly, B., Grivel-Gelly, C., Pérez, A., Socas-Navarro, H., Soltau, D., and Volkmer, R. (2010a). European Solar Telescope: project status. In *Ground-based and Airborne Telescopes III*, volume 7733 of *Proc. SPIE*, page 77330H.

Collados, M., Bettonvil, F., Cavaller, L., Ermolli, I., Gelly, B., Pérez, A., Socas-Navarro, H., Soltau, D., Volkmer, R., and EST Team (2010b). European Solar Telescope: Progress status. *Astronomische Nachrichten*, 331:615.

De Groot, S. R. and Mazur, P. (2013). *Non-equilibrium thermodynamics*. Courier Corporation.

Del Moro, D. (2004). Solar granulation properties derived from three different time series. *Astronomy and Astrophysics*, 428:1007–1015.

del Toro Iniesta, J. C. and Ruiz Cobo, B. (2016). Inversion of the radiative transfer equation for polarized light. *Living Reviews in Solar Physics*, 13:4.

Evans, D. J. and Searles, D. J. (2002). The Fluctuation Theorem. *Advances in Physics*, 51:1529–1585.

Forte, R., Berrilli, F., Calchetti, D., Del Moro, D., Fleck, B., Giebink, C., Giebink, W., Giovannelli, L., Heida, L., Jefferies, S. M., Knox, A., Magrì, M., Murphy, N., Nitta, G., Oliviero, M., Pietropaolo, E., Rodgers, W., Scardigli, S., and Viavattene, G. (2020). A Data Reduction Pipeline for MOF-based Synoptic Telescopes. *Journal of Space Weather and Space Climate*, 10.

Gallavotti, G. (1999). A local fluctuation theorem. *Physica A Statistical Mechanics and its Applications*, 263:39–50.

Gallavotti, G. and Cohen, E. G. D. (1995). Dynamical ensembles in stationary states. *Journal of Statistical Physics*, 80:931–970.

Getling, A. V. (2001). Rayleigh-bénard convection: structures and dynamics.

Giannattasio, F., Berrilli, F., Biferale, L., Del Moro, D., Sbragaglia, M., Bellot Rubio, L.,

Gošić, M., and Orozco Suárez, D. (2014a). Pair separation of magnetic elements in the quiet Sun. *A&A*, 569:A121.

Giannattasio, F., Berrilli, F., Consolini, G., Del Moro, D., Gošić, M., and Bellot Rubio, L. (2018). Occurrence and persistence of magnetic elements in the quiet Sun. *A&A*, 611:A56.

Giannattasio, F., Consolini, G., Berrilli, F., and Del Moro, D. (2019). The Complex Nature of Magnetic Element Transport in the Quiet Sun: The Lévy-walk Character. *ApJ*, 878(1):33.

Giannattasio, F., Del Moro, D., Berrilli, F., Bellot Rubio, L., Gošić, M., and Orozco Suárez, D. (2013). Diffusion of Solar Magnetic Elements up to Supergranular Spatial and Temporal Scales. *ApJ*, 770(2):L36.

Giannattasio, F., Stangalini, M., Berrilli, F., Del Moro, D., and Bellot Rubio, L. (2014b). Diffusion of Magnetic Elements in a Supergranular Cell. *ApJ*, 788(2):137.

Giovannelli, L., Berrilli, F., Calchetti, D., Del Moro, D., Viavattene, G., Pietropaolo, E., Iarlori, M., Rizi, V., Jefferies, S. M., Oliviero, M., Terranegra, L., and Murphy, N. (2020). The Tor Vergata Synoptic Solar Telescope (TSST): a robotic, compact facility for solar full disk imaging. *Journal of Space Weather and Space Climate*, 10.

Greco, V. and Cavallini, F. (2013). Optical design of a near-infrared imaging spectropolarimeter for the Advanced Technology Solar Telescope. *Optical Engineering*, 52:063001.

Gudiksen, B. V., Carlsson, M., Hansteen, V. H., Hayek, W., Leenaarts, J., and Martínez-Sykora, J. (2011). The stellar atmosphere simulation codebifrost. *Astronomy & Astrophysics*, 531:A154.

Guglielmino, S. L., Martínez Pillet, V., Bonet, J. A., del Toro Iniesta, J. C., Bellot Rubio, L. R., Solanki, S. K., Schmidt, W., Gandorfer, A., Barthol, P., and Knölker, M. (2012). The Frontier between Small-scale Bipoles and Ephemeral Regions in the Solar Photosphere: Emergence and Decay of an Intermediate-scale Bipole Observed with SUNRISE/IMaX. *ApJ*, 745(2):160.

Kaiser, A. and Schreiber, T. (2002). Information transfer in continuous processes. *Physica D: Nonlinear Phenomena*, 166:43–62.

Keil, S. L., Rimmele, T. R., and Wagner, J. (2009). Advanced Technology Solar Telescope. *Earth Moon and Planets*, 104:77–82.

Landi Degl'Innocenti, E. (2004). Fisica solare.

Landi Degl'Innocenti, E. and Landi Degl'Innocenti, M. (1985). On the solution of the radiative transfer equations for polarized radiation. *Sol. Phys.*, 97:239–250.

Landi Degl'Innocenti, E. and Landolfi, M., editors (2004a). *Polarization in Spectral Lines*, volume 307 of *Astrophysics and Space Science Library*.

Landi Degl'Innocenti, E. and Landolfi, M. (2004b). Polarization in spectral lines.

Levenberg, K. (1944). Quart. appl. math. 2, 164-168.

Löhner-Böttcher, J., Schmidt, W., Stief, F., Steinmetz, T., and Holzwarth, R. (2018). Convective blueshifts in the solar atmosphere. I. Absolute measurements with LARS of the spectral lines at 6302 Å. *A&A*, 611:A4.

Macaluso, D. and Corbino, O. M. (1898). Sopra una nuova azione che la luce subisce attraversando alcuni vapori metallici in un campo magnetico. *Il Nuovo Cimento*, 8(1):257–258.

Macaluso, D., Corbino, O. M., and Magri, L. (1899a). Sulla relazione tra il fenomeno di Zeemann e la rotazione magnetica anomala del piano di polarizzazione della luce. *Il Nuovo Cimento*, 9(1):384–389.

Macaluso, D., Corbino, O. M., and Magri, L. (1899b). Sulle modificazioni che la luce subisce attraversando alcuni vapori metallici in un campo magnetico. *Il Nuovo Cimento*, 9(1):381–384.

Marquardt, D. (1963). J. soc. indust. appl. math. 11, 431-441.

Martínez González, M. J. and Bellot Rubio, L. R. (2009). Emergence of Small-scale Magnetic Loops Through the Quiet Solar Atmosphere. *ApJ*, 700(2):1391–1403.

Niemela, J. J., Skrbek, L., Sreenivasan, K. R., and Donnelly, R. J. (2000). Turbulent

convection at very high Rayleigh numbers. *Nature*, 404(6780):837–840.

Nordlund, Å., Stein, R. F., and Asplund, M. (2009). Solar Surface Convection. *Living Reviews in Solar Physics*, 6(1):2.

Oliviero, M., Dolci, M., Severino, G., Straus, T., Cacciani, A., and Moretti, P. F. (1998a). VAMOS: Velocity and Magnetic Observations of the Sun. In Deubner, F.-L., Christensen-Dalsgaard, J., and Kurtz, D., editors, *New Eyes to See Inside the Sun and Stars*, volume 185 of *IAU Symposium*, page 53.

Oliviero, M., Moretti, P. F., Severino, G., Straus, T., Magrì, M., and Tripicchio, A. (2002). Preliminary Results on the Solar Photospheric Dynamics Observed with Vamos. *Sol. Phys.*, 209(1):21–35.

Oliviero, M., Severino, G., and Straus, T. (1998b). VAMOS: velocity and intensity data analysis and first results on I-V phase difference at low l. *Mem. Soc. Astron. Italiana*, 69:623.

Puschmann, K. G., Ruiz Cobo, B., Vázquez, M., Bonet, J. A., and Hanslmeier, A. (2005). Time series of high resolution photospheric spectra in a quiet region of the Sun. II. Analysis of the variation of physical quantities of granular structures. *Astronomy and Astrophysics*, 441(3):1157–1169.

Rast, M. (2015). Daniel K. Inouye Solar Telescope (DKIST) Critical Science Plan. *IAU General Assembly*, 22:2257167.

Rees, D. E. and Semel, M. D. (1979). Line formation in an unresolved magnetic element - A test of the centre of gravity method. *A&A*, 74:1–5.

Romano, P., Berrilli, F., Criscuoli, S., Del Moro, D., Ermolli, I., Giorgi, F., Viticchié, B., and Zuccarello, F. (2012). A Comparative Analysis of Photospheric Bright Points in an Active Region and in the Quiet Sun. *Sol. Phys.*, 280(2):407–416.

Ruiz Cobo, B. and del Toro Iniesta, J. C. (1992). Inversion of Stokes profiles. *ApJ*, 398:375–385.

Ruiz Cobo, B. and del Toro Iniesta, J. C. (1994). On the sensitivity of Stokes profiles to physical quantities. *A&A*, 283:129–143.

Sánchez Almeida, J., Bonet, J. A., Viticchié, B., and Del Moro, D. (2010). Magnetic Bright Points in the Quiet Sun. *ApJ*, 715(1):L26–L29.

Semel, M. (1967). Contribution à létude des champs magnétiques dans les régions actives solaires. *Annales d'Astrophysique*, 30:513–513.

Severino, G., Moretti, P. F., Oliviero, M., and Vamos Team (2001). The Velocity And Magnetic Observations of the Sun (VAMOS) project: status and future prospects. In Wilson, A. and Pallé, P. L., editors, *SOHO 10/GONG 2000 Workshop: Helio- and Asteroseismology at the Dawn of the Millennium*, volume 464 of *ESA Special Publication*, pages 337–340.

Shang, X.-D., Tong, P., and Xia, K.-Q. (2005). Test of steady-state fluctuation theorem in turbulent Rayleigh-Bénard convection. *Phys. Rev. E*, 72(1):015301.

Socas-Navarro, H. (2015). NICOLE: NLTE Stokes Synthesis/Inversion Code. Astrophysics Source Code Library.

Socas-Navarro, H., de la Cruz Rodríguez, J., Asensio Ramos, A., Trujillo Bueno, J., and Ruiz Cobo, B. (2015). An open-source, massively parallel code for non-LTE synthesis and inversion of spectral lines and Zeeman-induced Stokes profiles. *A&A*, 577:A7.

Socas-Navarro, H., Ruiz Cobo, B., and Trujillo Bueno, J. (1998). Non-LTE Inversion of Line Profiles. *ApJ*, 507:470–481.

Socas-Navarro, H., Trujillo Bueno, J., and Ruiz Cobo, B. (2000). Non-LTE Inversion of Stokes Profiles Induced by the Zeeman Effect. *ApJ*, 530:977–993.

Stangalini, M., Viticchiè, B., Del Moro, D., Piazzesi, R., and Berrilli, F. (2009). Spectropolarimetry with IBIS at NSO/DST: Evolution of Bright Points in the Quiet Sun. In *AGU Fall Meeting Abstracts*, page SH51A.

Stein, R. F. (2012). Solar Surface Magneto-Convection. *Living Reviews in Solar Physics*, 9(1):4.

Tritschler, A., Rimmele, T. R., Berukoff, S., Casini, R., Craig, S. C., Elmore, D. F., Hubbard, R. P., Kuhn, J. R., Lin, H., McMullin, J. P., Reardon, K. P.,

Schmidt, W., Warner, M., and Woger, F. (2015). DKIST: Observing the Sun at High Resolution. In van Belle, G. T. and Harris, H. C., editors, *18th Cambridge Workshop on Cool Stars, Stellar Systems, and the Sun*, volume 18 of *Cambridge Workshop on Cool Stars, Stellar Systems, and the Sun*, pages 933–944.

Viavattene, G., Berrilli, F., Collados Vera, M., Del Moro, D., Giovannelli, L., Ruiz Cobo, B., and Zuccarello, F. (2018). Remote sensing of the solar photosphere: a tale of two methods. In *Journal of Physics Conference Series*, volume 956 of *Journal of Physics Conference Series*, page 012006.

Viavattene, G., Berrilli, F., Consolini, G., Del Moro, D., Giannattasio, F., Giovannelli, L., and Penza, V. (2019a). Evaluating a proxy of the local entropy production rate on the solar photosphere. In *Journal of Physics Conference Series*, volume 1226 of *Journal of Physics Conference Series*, page 012004.

Viavattene, G., Berrilli, F., Consolini, G., Del Moro, D., Giannattasio, F., Giovannelli, L., and Penza, V. (2019b). Statistical behaviour of a proxy of the entropy production rate of the solar photosphere. *Nuovo Cimento C Geophysics Space Physics C*, 42(1):8.

Viavattene, G., Calchetti, D., Berrilli, F., Del Moro, D., Giovannelli, L., Pietropaolo, E., Oliviero, M., and Terranegra, L. (2020a). Optical design of the tor vergata synoptic solar telescope (tsst). *Nuovo Cimento della Societa Italiana di Fisica C*, 43(4-5).

Viavattene, G., Consolini, G., Giovannelli, L., Berrilli, F., Del Moro, D., Giannattasio, F., Penza, V., and Calchetti, D. (2020b). Testing the Steady-State Fluctuation Relation in the Solar Photospheric Convection. *Entropy*, 22(7):716.

Viavattene, G., Zuccarello, F., Collados Vera, M., and Ruiz Cobo, B. (2019c). Spectropolarimetric analysis of a short lived solar active region. *Nuovo Cimento C Geophysics Space Physics C*, 42(1):10.

Viticchié, B. (2012). On the Polarimetric Signature of Emerging Magnetic Loops in the Quiet Sun. *ApJ*, 747(2):L36.

Viticchiè, B., Del Moro, D., Berrilli, F., Rubio, L. B., and Tritschler, A. (2011). IBIS 2D Spectropolarimetry: Analysis of G-band Bright Points. In Kuhn, J. R., Harrington, D. M., Lin, H., Berdyugina, S. V., Trujillo-Bueno, J., Keil, S. L., and Rimmele, T., editors, *Solar Polarization 6*, volume 437 of *Astronomical Society of the Pacific Conference Series*, page 75.

Viticchié, B., Del Moro, D., Criscuoli, S., and Berrilli, F. (2010). Imaging Spectropolarimetry with IBIS. II. On the Fine Structure of G-band Bright Features. *ApJ*, 723:787–796.

Vögler, A., Shelyag, S., Schüssler, M., Cattaneo, F., Emonet, T., and Linde, T. (2005). Simulations of magneto-convection in the solar photosphere. Equations, methods, and results of the MURaM code. *A&A*, 429:335–351.

Wilken, V., de Boer, C. R., Denker, C., and Kneer, F. (1997). Speckle measurements of the centre-to-limb variation of the solar granulation. *Astronomy and Astrophysics*, 325:819–824.

Woeger, F. (2016). The DKIST Instrumentation Suite. In *AAS/Solar Physics Division Abstracts #47*, volume 47 of *AAS/Solar Physics Division Meeting*, page 201.02.

Zuccarello, F. and EST Team (2012). The European Solar Telescope: project status . *Memorie della Societa Astronomica Italiana Supplementi*, 19:67.